Mechanical analysis of widespread corrosion-damaged structure based on ES-PIM

†Keliang Ren, *Jimin Li[1], Hua Ji[2] ,Ting Wang[3] ,Lihong Ding[4] and Jia Yang[5]

† Department of physics and electrical and electronic engineering, Ningxia University, P. R. China

[1,3,5]Department of physics and electrical and electronic engineering, Ningxia University, P. R. China

[2]College of Mechanical Engineering, Ningxia University, P. R. China

[4]Department of mathematics and statistics, Ningxia University, P. R. China

*Presenting author: liangliang910201@126.com

†Corresponding author: kl_ren@nxu.edu.cn

Abstract

In order to solve the problem of large limitation of simulation results caused by load factors and corrosion conditions respectively in the study of corrosion failure of metallic materials, the idea of combining cellular automata and edge-based smoothed point interpolation method (ES-PIM) is adopted. The corrosion process of aluminum under environmental action was simulated by cellular automata method and the corrosion topography was obtained which was used for the establishment of calculation model. To overcome overly-stiff property existing in the widely used finite element method (FEM) with linear triangular elements, the edge-based smoothed point interpolation method (ES-PIM) is used for calculation which has been found both spatially and temporally stable, and works well for both static and dynamic problems.

Keywords: Widespread corrosion damage Cellular Automaton Meshfree method

1.Introduction

As a kind of nonferrous metal structural materials, aluminum and its alloys are widely used in aviation, aerospace, automobile, machinery manufacturing and so on. In the process of its use, it will suffer different forms of damage due to the influence of the service environment, among which corrosion is a common form of damage. However, the failure of aluminum structure is not caused by the single factor of corrosion, usually accompanied by the action of load on it. Most scholars have simulated the corrosion behavior of aluminum based on the corrosion mechanism of aluminum, but have not carried out mechanical analysis on the corrosion defect structure generated subsequently. Therefore, it is of great significance to simulate the corrosion and failure behavior of aluminum and its alloys in the service environment.

In the field of aluminum corrosion behavior simulation, Engelhardt et al.[1-3] established a damage function analysis model to predict local corrosion such as pitting corrosion, crevice corrosion and stress corrosion. Urquidi-macdonald et al.[4] studied the relationship between the crack growth rate caused by pitting corrosion and various parameters (corrosion potential, pH, temperature and conductivity) using artificial neural network technology (ANN).In Cellular Automata (CA) model, space is divided into cells with finite states. These cells

evolve according to certain local rules. By the CA model based on the rules of local reactions in the system, can reflect the influence of different scales complex physical and chemical systems, by defining the molecular scale or the interaction of the atomic scale, within the scope of the macro qualitatively describe the nature of the complex system, so using the CA technology to rot corrosion in the process modeling more intuitive and convenient, like Wang Hui et al. [5-6] adopted cellular automata (CA) method to obtain the growth and evolution curve of corrosion pits and the change curve of geometric morphology with time.

After years of development, finite element method (FEM) has become an important tool for modeling and simulation of solid and complex geometric structures. However, the finite element method has some inherent defects. For example, the finite element model is "overly-stiff", which affects the accuracy of strain, especially for stress results; When the mesh is severely deformed, the precision of the solution will be affected.

During mesh generation, using triangle (for 2D) or tetrahedron (for 3D) elements, mesh generation becomes much easier and is usually done automatically without manual manipulation. But at the same time, the accuracy of finite element calculation results is often very poor.

Professor G.R. LIU[7-9]and his team used point-based polynomial interpolation (PIM)[10] or radial basis interpolation(RPIM)[11] to construct the shape function, and introduced smoothed Galerkin weakform and generalized gradient smooth operator [12,13]. Thus, the node-based smoothed point interpolation method [14,15](NS-PIM) can be obtained.

In practical application, this method shows that it can withstand mesh deformation better and still has good calculation results under triangular mesh. Moreover, this method provides the upper bound of energy norm. However, the stiffness matrix **K** obtained by this method is smaller than the actual stiffness matrix **K**, that is, the smoothed system is "overly-soft", resulting in a displacement larger than the actual displacement. In order to solve this problem, Edge-based smoothed Point Interpolation Method[16-18] (ES-PIM) is introduced.

In ES-PIM, every edge-related problem domain of the background grid is smoothed. Compared with the node-based smooth operator, the smoothness of edge-basis strain can weaken the degree of softening, so that the ES-PIM model is closer to the exact stiffness and has a good calculation effect in both static and dynamic problems.

For the above methods, professor G.R.LIU and his team established Galerkin weakened weak (W^2) formulation constructed by generalized gradient smoothing operator.

Weakened weak (W^2) formulation seeks solutions in G space[19]which is a function space containing both continuous and discontinuous functions. G space includes all the continuous and discontinuous displacement cases under the framework of FEM and Meshfree. Therefore, in the framework of finite element and meshless method, it is suitable for both compatible and incompatible displacements. By using the generalized strain smoothing technique, we can

obtain the generalized smooth Galerkin weak form for all the above methods.

In this paper, the widespread corrosion behavior of aluminum is simulated by using cellular automata method, and a computational model is established based on the simulated corrosion topography. The model is analyzed by introducing edge-based smoothed point interpolation method and the results are obtained. The combination of the two methods provides a new way to analyze the mechanical properties of structures with corrosion defects.

2. Establishment of widespread corrosion model

2.1 Definition of cellular automata

Cellular Automata (CA) is defined as a dynamic system that evolves in discrete time dimensions in accordance with certain local rules in a cellular space composed of cells with discrete and finite states.

In the process of its evolution, each cell can change according to local rules state, namely based on cellular automata and its neighbor cell state with this to determine the next state of cellular automata, all belong to sync status updates, in accordance with local rules the entire cellular space show the change of state in discrete time.

2.2 Boundary conditions

When simulating a given cellular automata rule, one cannot deal with an infinite lattice. The system must be finite and have boundaries. Clearly, a site belonging to the lattice boundary does not have the same neighborhood as other internal sites. In order to define the behavior of these sites, a different evolution rule can be considered, which sees the appropriate neighborhood. This means that the information of being, or not, at a boundary is coded at the site and, depending on his information, a different rule is selected.

Each variable of cellular automata has a finite number of states and is local in time and space. In order to keep each variable in the cellular space free from the influence of the external environment, the boundary conditions of the model are usually defined as follows: Periodic boundary conditions are used for the left and right boundary to keep the properties of the system and the element unchanged, and the theoretical infinity of cellular space is realized. The upper and lower boundaries adopt fixed boundary conditions to ensure the non-correlation of upper and lower boundary cells, as shown in Figure 1.

A cellular automata rule is local, by definition. The updating of a given cell requires one to know only the state of the cells in its vicinity. The spatial region in which a cell needs to search is called the neighborhood. In principle, there is no restriction on the size of the neighborhood, except that it is the same for all cells. However, in practice, it is often made up of adjacent cells only. If the neighborhood is too large, the complexity of the rule may be unacceptable (complexity usually grows exponentially fast with the number of cells in the neighborhood).

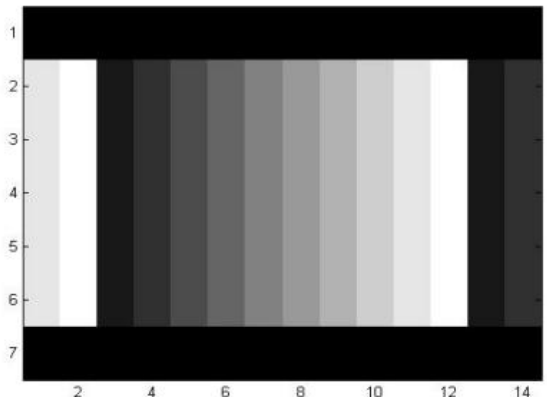

Figure 1. Schematic Diagram of boundary conditions

For two-dimensional cellular automata, two neighborhoods are often considered: the von Neumann neighborhood, which consists of a central cell (the one which is to be updated) and its four geographical neighbors north, west, south and east. The Moore neighborhood contains, in addition, second nearest neighbors northeast, northwest, southeast and southwest, that is a total of nine cells.[7]

Figure 2. illustrates these two standard neighborhoods.

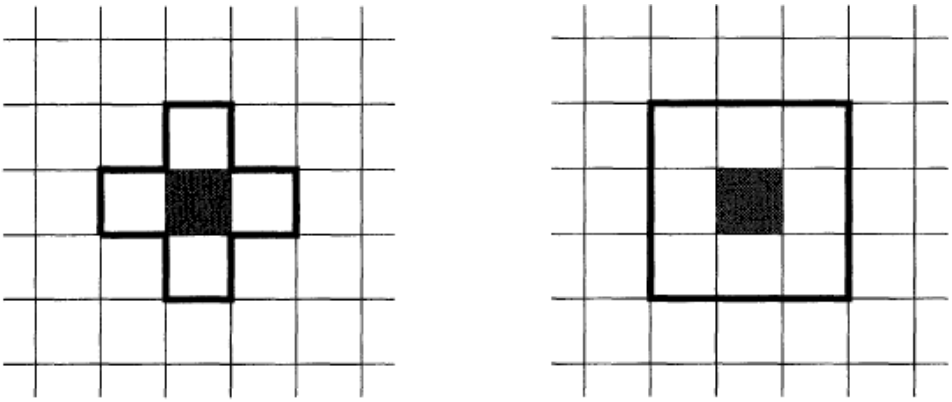

(a) (b)

Figure 2. (a) Von Neumann and (b) Moore neighborhoods. The shaded region indicates the central cell which is updated according to the state of the cells located within the domain marked with the bold line.

2.3 transformation rule

In the study on the formation process of metal corrosion products, the cellular transformation process is realized, which is expressed by the following conversion equation:

$$M + C \rightarrow P \tag{1}$$

In the top formula, M is the metal cell; C is corrosive cell; P is the cell of corrosion product. In particular, the concentration of oxygen in the atmosphere changes very little, and the key factor affecting the corrosion rate of metal oxygen absorption is the relative humidity of water molecules. Therefore, in order to simplify the CA model, only water molecules involved in the reaction are represented by C in the equation, and the effect of oxygen on corrosion is no

longer considered.

Cellular conversion rules: only corrosion cell C in cellular space has random mobility (top, bottom, left, right). If C moves in the direction of neighbor metal cell M, both M and C are converted to P. Conversely, if the neighbor is C, all cells remain unchanged. If the neighbor in the direction of C is a space bit, then C will jump to the space bit, and the original position will randomly become a space bit; If all neighbors of M are C, all cells remain unchanged. If at least one neighbor of M is C, and C does not move toward M, M also remains unchanged.

3. Numerical model

3.1 Brief on Basic Equations

The stress-strain problem of corrosion-damaged structure belongs to the linear elastic problem of solid mechanics, so we first brief the basic equations for solid mechanics problem of linear elasticity.

Consider a two-dimensional solid mechanics problem with a physical domain of $\Omega \in R^2$ bounded by Γ.The static equilibrium equation for 2D solids in the domain $\Omega \in R^2$ can be written as:

$$\frac{\partial \sigma_{ij}}{\partial x_j} + b_i = 0, \qquad i, j = 1, 2 \tag{2}$$

where b_i are given external body force and σ_{ij} is the stress tensor which relates to the strains tensor ε_{ij} via the constitutive equation or the Generalized Hook's law:

$$\sigma_{ij} = C_{ijkl}\varepsilon_{kl} \tag{3}$$

where C_{ijkl} is elasticity tensor of material property constants.

The strains tensor ε_{ij} relates to the displacement by the following compatibility equation.

$$\varepsilon_{kl} = \frac{1}{2}\left(\frac{\partial u_k}{\partial x_l} + \frac{\partial u_l}{\partial x_k} \right) \tag{4}$$

where u_i, $i = 1, 2$ is the displacement components in the xi-directions at a point in Ω .

In matrix form, the equilibrium Eq.(2) becomes:

$$\mathbf{L}_d \boldsymbol{\sigma} + \mathbf{b} = 0 \tag{5}$$

where $\mathbf{L}_d$ is a matrix of the differential operator defined as:

$$\mathbf{L}_d\left(\frac{\partial}{\partial x_1}, \quad \frac{\partial}{\partial x_2} \right) = \begin{bmatrix} \dfrac{\partial}{\partial x_1} & 0 \\ 0 & \dfrac{\partial}{\partial x_2} \\ \dfrac{\partial}{\partial x_2} & \dfrac{\partial}{\partial x_1} \end{bmatrix} \tag{6}$$

The constitutive equation becomes:

$$\boldsymbol{\sigma} = \mathbf{C}\boldsymbol{\varepsilon} \tag{7}$$

Where $\mathbf{C}$ is matrix of material properties which entries of C_{ijkl} , $\boldsymbol{\sigma} = \{\sigma_{11} \quad \sigma_{22} \quad \sigma_{12}\}^T$ and $\boldsymbol{\varepsilon} = \{\varepsilon_{11} \quad \varepsilon_{22} \quad \varepsilon_{\mathrm{r}2}\}^T$

The compatibility equation (4) can also be written in the matrix form of :

$$\boldsymbol{\varepsilon} = \mathbf{L}_d \mathbf{u} \tag{8}$$

where $\mathbf{u} = \{u_1 \quad u_2\}^T$ is the displacement vector. Substituting Eq.(8) into (7) and then into (5):

$$\mathbf{L}_d^T \mathbf{C} \mathbf{L}_d \mathbf{u} + \mathbf{b} = \mathbf{0} \tag{9}$$

There are two types of boundary conditions: Dirichlet (or essential / displacement) boundary conditions and Neumann (or natural / stress) boundary conditions. Let Γ_D denote a part of Γ , on which homogenous Dirichlet boundary condition is specified, then we can obtain:

$$\Gamma_D \in \Gamma \quad \text{on} \quad u_i = 0, \tag{10}$$

Let Γ_N denotes a part of Γ , on which Neumann boundary condition is satisfied,

$$\sigma_{ij} n_j = t_i, \quad \text{on} \quad \Gamma_N \in \Gamma \tag{11}$$

where n_j is unit outward normal vector, and t is the specified boundary stress on Γ_N , respectively. The matrix form of Eq.(11) is as follows:

$$\mathbf{L}_n^T \sigma = \mathbf{t}, \quad \text{on} \quad \Gamma_N \in \Gamma \tag{12}$$

Where

$$\mathbf{L}_n \begin{pmatrix} n_x & n_y \end{pmatrix} = \begin{bmatrix} n_x & 0 \\ 0 & n_y \\ n_y & n_x \end{bmatrix} \tag{13}$$

3.2 Displacement field approximation using the PIM

The point interpolation method (PIM) obtains the approximation by letting the interpolation function pass through the function values at each scattered node within the local supporting domain.

Different types of point interpolation can be constructed by using different types of base functions. There are two common types: Polynomial point interpolation method (PIM) based on polynomial basis function and radial point interpolation method (RPIM) based on radial basis function.

For the polynomial PIM, the formulations start with the following assumption:

$$u(x) = \sum_{i=1}^{n} P_i(\mathbf{x}) a_i = \mathbf{P}^T(\mathbf{x})\mathbf{a} \tag{14}$$

Where $u(x)$ is a field variable function defined in the Cartesian coordinate space $\mathbf{x}^T = \{x \quad y\}$, $P_i(\mathbf{x})$ is the basis function of monomials which is usually built utilizing Pascal's triangles, a_i is the corresponding coefficient, and n is the number of nodes in the local support domain. The complete polynomial basis of orders 1 and p can be written as:

$$\mathbf{P}^T(\mathbf{x}) = \begin{pmatrix} 1 & x & x^2 & \cdots & x^p \end{pmatrix}, \quad 1D \tag{15}$$

$$\mathbf{P}^T(\mathbf{x}) = \begin{pmatrix} 1 & x & y & x^2 & xy & \cdots & x^p & y^p \end{pmatrix}, \quad pD \tag{16}$$

For the radial PIM, using radial basis functions augmented with polynomials, the field function can be approximated as follows:

$$u(x) = \sum_{i=1}^{n} R_i(\mathbf{x}) a_i + \sum_{j=1}^{m} P_i(\mathbf{x}) b_j = \mathbf{R}^T(\mathbf{x})\mathbf{a} + \mathbf{P}^T(\mathbf{x})\mathbf{b} \tag{17}$$

Where $R_i(\mathbf{x})$ and $P_j(\mathbf{x})$ are radial basis functions and polynomial basis functions respectively, a_i and b_j are corresponding coefficients, n is the number of nodes in the local support domain and m is the number of polynomial terms.

The coefficients in Eqs.(14) and (17) can be determined by enforcing the field function to be satisfied at the n nodes within the local support domain. Finally, the PIM shape functions can be obtained and the field function can be expressed as:

$$u(\mathbf{x}) = \sum_{i=1}^{n} \varphi_i(\mathbf{x}) d_i = \mathbf{\Phi}^T(\mathbf{x})\mathbf{d} \tag{18}$$

where d_i is a nodal function value and $\varphi_i(\mathbf{x})$ is the PIM shape function which possesses the Kronecker delta function property. In the above formulation, it is noticed that we need to properly select n nodes for interpolation ensuring a nonsingular moment matrix.

3.3 T schemes for node selection

In this paper, three-point triangular background element is adopted to discretize the problem domain. The element can be generated automatically without manual operation, and the mesh density of triangular background element can be adjusted according to the need of computational accuracy.

The T scheme used in ES-PIM method mainly includes T3 scheme, T6/T3 scheme and T6 scheme. The following mainly introduce the T3 and T3/T6 scheme which used for programming.

The T3 scheme mainly uses the three vertices of the triangular mesh where the calculation point is located to represent the displacement function of the calculation point, and its displacement field is a linear displacement field. This method has many similarities with the first-order finite element interpolation method. The T3 scheme is used only for creating linear PIM shape functions by using polynomial basis functions. As illustrated in Figure 3.

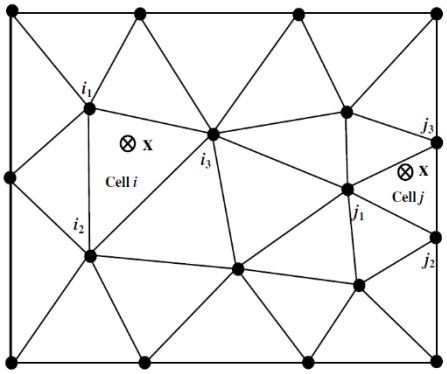

Figure 3. Illustration of the T3 scheme of node selection

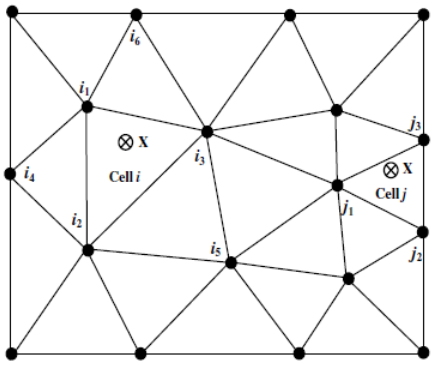

Figure 4. Illustration of the T6/T3 scheme of node selection

Whether the point of interest $(\mathbf{x})$ is located in an interior cell (element i) or a boundary cell (element j), only the three nodes of the home cell ($i_1 - i_3$ or $j_1 - j_3$) are selected.

In the T6/T3 scheme, the point of interest located in the boundary cell only needs three nodes to interpolate and the linear displacement approximation function also constructed by these three nodes. For the point of interest located in an interior cell needs six nodes to interpolate and been used for construct a quadratic displacement approximation function. As illustrated in Figure 4.

It not only successfully overcomes the singular problem which exists in the process of PIM approximation by using the polynomial basis but also improves the efficiency of the method.

3.4 Edge-based smoothed strains

In consideration of the displacement field is not continuous, the generalized smoothed Galerkin weak form or the weakened weak form which has exactly the same form as the standard Galerkin weak form need to be used.

$$\int_\Omega \delta\left(\hat{\varepsilon}\left(\mathbf{u}\right)\right)^T \mathbf{D}\left(\hat{\varepsilon}\left(\mathbf{u}\right)\right) d\Omega - \int_\Omega \delta\mathbf{u}^T \mathbf{b} d\Omega - \int_{\Gamma_t} \delta\mathbf{u}^T \mathbf{t} d\Gamma = 0 \tag{19}$$

Thus, the formulation procedure is exactly the same as that in the standard FEM and all we need to do is to use the edge-based smoothed strain $\hat{\varepsilon}$ in place of the compatible strain fields $\tilde{\varepsilon}$.

In the framework of W² formulation, the gradient of the field function (strains) will be obtained using the following generalized smoothing operation which considers both continuous and discontinuous displacement functions.[20]

$$\hat{\varepsilon}_k = \begin{cases} \dfrac{1}{A_k}\int_{\Omega_k} \tilde{\varepsilon}(x) d\Omega = \dfrac{1}{A_k}\int_{\Gamma_k} \mathbf{L}_n \mathbf{u}(x) d\Gamma & \textit{When } \mathbf{u}(x) \textit{ is continuous in } \Omega_k \\ \dfrac{1}{A_k}\int_{\Gamma_k} \mathbf{L}_n \mathbf{u}(x) d\Gamma & \textit{When } \mathbf{u}(x) \textit{ is discontinuous in } \Omega_k \end{cases} \tag{20}$$

where $\tilde{\varepsilon}$ is the compatible strain, $\hat{\varepsilon}_k$ is the smoothed strain over the smoothing domain(Ω_k),

A_k is the area and Γ_k is the boundary of the smoothing domain Ω_k.

To perform the generalized strain smoothing, the problem domain is first discretized using three-node triangular background cells, and then the stationary and nonoverlapping smoothing domains are constructed based on these triangles such that $\Omega = \Omega_1 \cup \cdots \cup \Omega_{N_S}$ and $\Omega_i \cap \Omega_j = \varnothing, i \neq j$ in which N_S is the number of smoothing domains.

Under the framework of ES-PIM theory the, smoothing domains are constructed for the edges of triangular cells by connecting two ends of the edge to the centroids of two adjacent cells. As illustrated in Figure 5. Thus, the number of smoothing domains (N_S) equals the number of edges of triangles (N_{edge}).

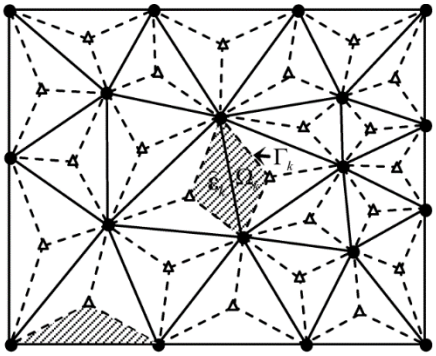

Figure 5. Construction of edge-based strain smoothing domains, which are stationary, nonoverlapping and constructed based on the three-node triangular cells.

Substituting Eq. (8) into Eq. (20), the edge-based smoothed strain $\hat{\varepsilon}_k$ can be written in the following matrix form of nodal displacements:

$$\hat{\varepsilon}_k = \frac{1}{A_k}\int_{\Gamma_k} \mathbf{L}_n \mathbf{\Phi} \mathbf{d}_i d\Gamma = \sum_{i \in N_{\text{infl}}} \hat{\mathbf{B}}_i(\mathbf{x}_k)\mathbf{d}_i \tag{21}$$

where $\mathbf{\Phi}$ is the matrix of PIM shape functions and N_{infl} is the number of field nodes involved in constructing the smoothed strain fields within Ω_k. $\hat{\mathbf{B}}_i(\mathbf{x}_k)$ is termed the smoothed strain matrix, which can be expressed as:

$$\hat{\mathbf{B}}_i(\mathbf{x}_k) = \begin{bmatrix} \hat{\mathbf{b}}_{ix}(\mathbf{x}_k) & 0 \\ 0 & \hat{\mathbf{b}}_{iy}(\mathbf{x}_k) \\ \hat{\mathbf{b}}_{iy}(\mathbf{x}_k) & \hat{\mathbf{b}}_{ix}(\mathbf{x}_k) \end{bmatrix} \tag{22}$$

In the above equation, elements of the smoothed strain matrix are obtained as:

$$\hat{\mathbf{b}}_{il}(\mathbf{x}_k) = \frac{1}{A_k}\int_{\Gamma_k} \varphi_i(\mathbf{x}_k) n_l(\mathbf{x}_k) d\Gamma \qquad (l = x, y) \tag{23}$$

Using the Gauss integration scheme, the above integration can be further expressed as follows:

$$\hat{\mathbf{b}}_{il} = \frac{1}{A_k}\sum_{m=1}^{N_{seg}} \left[\sum_{n=1}^{N_{Gauss}} w_n \varphi_i(\mathbf{x}_{mn}) n_i(\mathbf{x}_m) \right] \qquad (l = x, y) \tag{24}$$

where N_{seg} is the number of segments of the boundary Γ_k , N_{Gauss} is the number of Gauss points which located in each segment on Γ_k , and w_n is the corresponding weight number of the Gauss integration scheme.

By using the PIM with different T schemes we can construct the displacement field. Then, substituting the assumed displacements and the smoothed strains which given by Eq.(20) into Eq.(19), a set of discretized algebraic system equations can be obtained in the matrix form:

$$\hat{\mathbf{K}}\mathbf{d} = \hat{\mathbf{f}} \tag{25}$$

$\hat{\mathbf{f}}$ is the force vector, which can be obtain as:

$$\hat{\mathbf{f}} = -\int_{\Omega} \mathbf{\Phi}^T \mathbf{b} d\Omega + \int_{\Gamma_t} \mathbf{\Phi}^T \mathbf{t}_{\Gamma} d\Gamma \tag{26}$$

and the stiffness matrix $\hat{\mathbf{K}}$ is assembled from the substiffness matrix for all the integration cells which are exactly the edge-based smoothing domains for the present method:

$$\hat{\mathbf{K}}_{ij} = \sum_{k=1}^{N_a} \hat{\mathbf{K}}_{ij(k)} \tag{27}$$

where $\hat{\mathbf{K}}_{ij}$ is the substiffness matrix associated with the integration cell k (i.e. smoothing domain Ω_k), which is computed using the smoothed strain matrix, as follows:

$$\hat{\mathbf{K}}_{ij(k)} = \int_{\Omega_k} \hat{\mathbf{B}}_i^T D \hat{\mathbf{B}}_j d\Omega \tag{28}$$

4. The Solution of widespread corrosion-damaged structure

In the service environment, corrosion damage of engineering structures are usually not just single point corrosion damage, instead, widespread corrosion is the main form of structural corrosion. The occurrence of widespread corrosion is often random, which makes the cellular automata method more suitable for simulation

4.1 Establishment of widespread corrosion-damaged structure model

In order to simulate the formation process of widespread corrosion, we use cellular automata method combined with MATLAB software for programming. The morphological model of widespread corrosion-damaged structure of aluminum can be obtained by simulation program. As illustrated in Figure 6.

Figure 6. Topography of widespread corrosion damage structures

Where the black part in Fig.6 is the appearance of the corroded aluminum metal, with Young's modulus $E = 7.1\times10^{10}\,\mathrm{Pa}$ and Poisson's ratio $\nu = 0.33$, the white part is the liquid with a certain concentration of corrosion and causes widespread corrosion defects on the surface of aluminum. There are two main factors influencing corrosion morphology, one is relative humidity, the other is ambient temperature.Figure.6 shows the widespread corrosion-damaged structure morphology which forms in relative humidity 70% and the temperature of 50℃.

The solution domain was determined based on the simulated widespread corrosion morphology, and the computational model was established by combining Fortran programming, as illustrated in Figure 7.

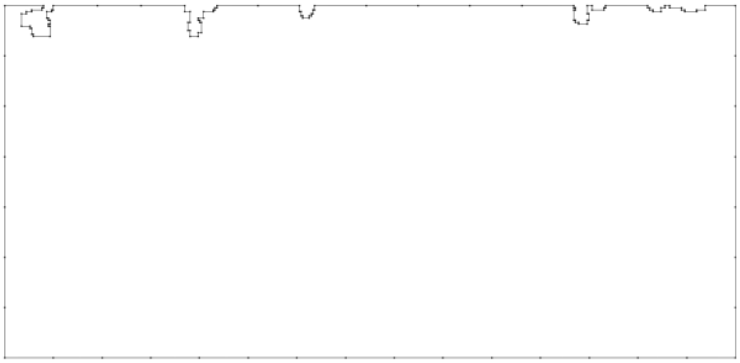

Figure 7. Calculation model of widespread corrosion morphology

Hinge constraints are applied to the left edge of the member containing widespread corrosion-damaged, and 15kN distributed load is applied to the right edge for stretching.

The problem domain and its boundary are modelled and represented by using 35920 nodes scattered in the problem domain and on its boundary. The density of the nodes depends on the accuracy required and resources available.

Near the upper edge of the corrosion morphological structure model, we use adaptive algorithms to improve the computational accuracy. As illustrated in Figure 8.

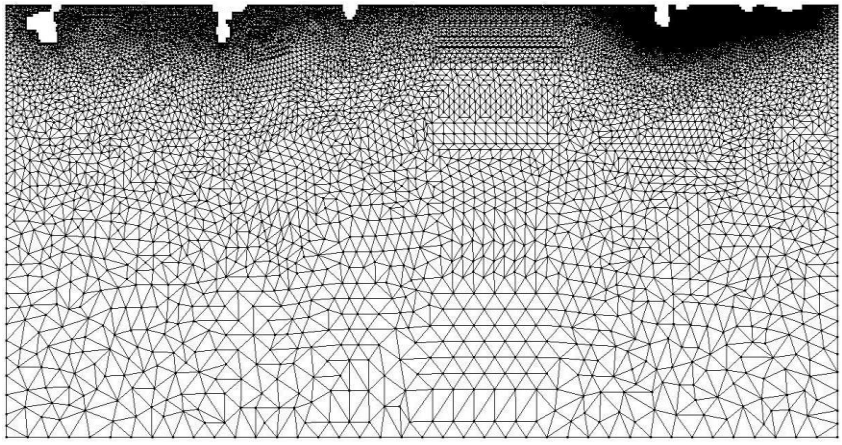

Figure 8. Domain discretization of the widespread corrosion-damaged structure by using 35920 nodes and 70065 triangular meshes.

4.2 The solution of the widespread corrosion structure

The results of stresses obtained using ES-PIM are listed in Tables 1.

Table 1. The output sample for stress obtained

No. of field nodes	σ_{xx}	σ_{yy}	τ_{xy}
1	4.78E+03	1.90E+02	-3.75E+02
2	4.80E+03	-1.12E+03	2.02E+03
3	8.34E+03	1.15E+03	-2.40E+03
4	5.24E+03	-1.56E+02	-2.18E+03
5	4.55E+03	-1.13E+03	-2.73E+03
6	4.37E+03	-1.62E+03	-2.90E+03
7	4.85E+03	-1.54E+03	-3.13E+03
8	5.93E+03	-1.70E+03	-3.72E+03
9	6.57E+03	-1.87E+03	-4.03E+03
10	7.78E+03	-1.56E+03	-4.45E+03
⋮			
35918	1.08E+04	-1.20E+03	3.15E+03
35919	2.81E+04	4.76E+03	-2.05E+03
35920	9.42E+03	-7.85E+02	1.29E+03

The distribution of stresses in the domain obtained by ES-PIM are drawn by Tecplot shown in Figure 9. respectively.

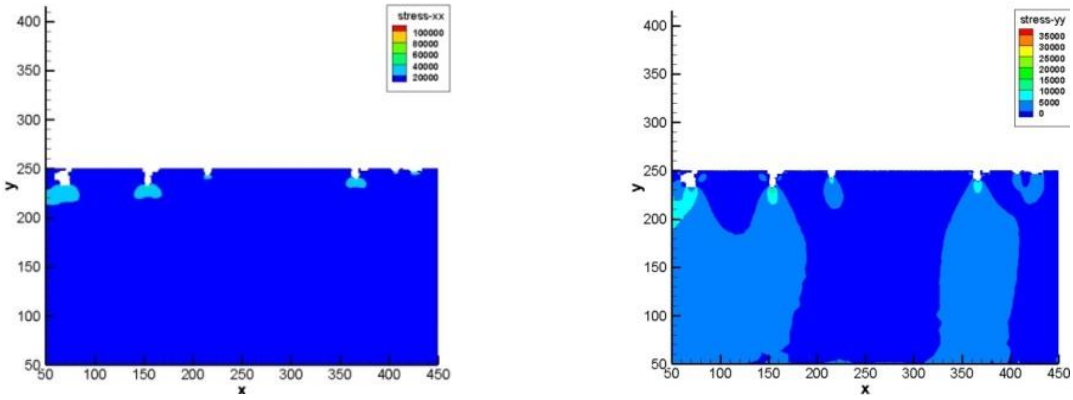

(a) (b)

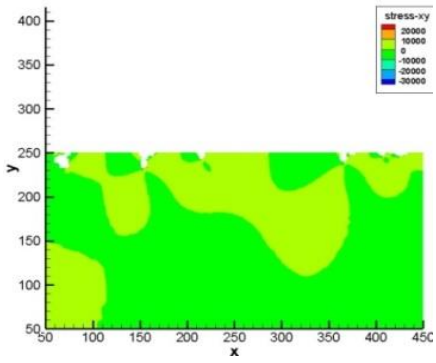

(c)

Figure 9. (a), (b), (c) are stress nephogram of σ_{xx},σ_{yy} and τ_{xy} respectively.

The results of displacements obtained using ES-PIM are listed in Tables 2.

Table 2. The output sample for strain obtained

No. of field nodes	u	v
1	4.75E+03	2.21E+02
2	4.00E+03	-3.21E+02
3	7.42E+03	2.07E+03
4	4.13E+03	9.55E+02
5	2.51E+03	9.14E+02
6	2.11E+03	6.34E+02
7	2.29E+03	1.02E+03
8	2.94E+03	1.28E+03
9	3.61E+03	1.08E+03
10	4.53E+03	1.69E+03
⋮		
35919	2.79E+04	4.94E+03
35920	9.25E+03	-6.19E+02

The distribution of stresses in the domain obtained by ES-PIM are drawn by Tecplot shown in Figure 10. respectively.

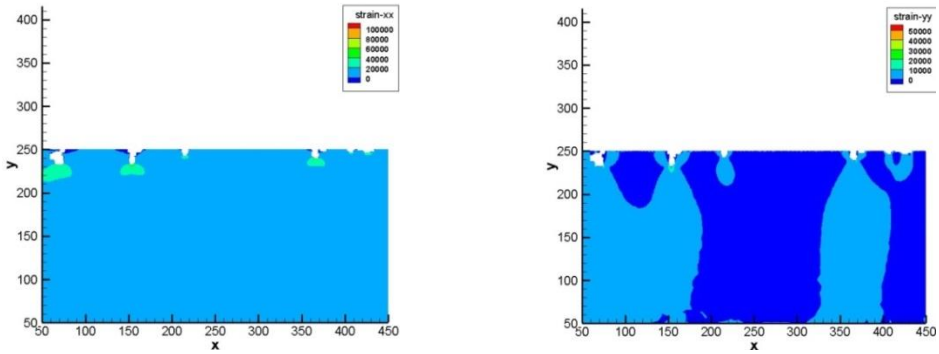

(a) (b)

Figure 10. (a), (b) are strain n ephogram of u and v respectively.

5. Conclusions and discussions

In this work, an edge-based point interpolation method for widespread corrosion-damaged structure problems is formulated. And it provides a new way to solve the problem of widespread corrosion-damaged structure and lays a foundation for the research of integrated disruption of corrosion structure. The following conclusions can be drawn from the analysis:

The PIM shape functions used in the ES-PIM have the Kronecker delta function property. Thus, we can perform the straightforward imposition of point essential boundary conditions and no additional treatments are needed to apply continuity conditions along the interface to meet the interface condition. For the present ES-PIM models, the requirement for the nodes distribution and mesh generation along the interface is exactly the same as that for the FEM.

The influence range of stress concentration of corrosion pits with relatively close distance is wider than that of a single corrosion pit, therefore, the widespread corrosion damage structure is more likely to generate cracks in the stress concentration area and eventually lead to the failure of the structure.

References

[1] Engelhardt G, Macdonald D D, Urquidi-Macdonald M. Development of fast algorithms for estimating stress corrosion growth rate [J] Corrosion Science, 1999, 41(12):2267-2302.

[2] Engelhardt G, Macdonald D D. Deterministic prediction of pit depth distribution [J]. Corrosion, 1998,54(6):469-479

[3] Macdonald D D, Engelhardt G. Deterministic prediction of localized corrosion damage a reflective review of critical issues[J]. Journal of Corrosion Science and Engineering, 2003, 6:C066.

[4] LU P C, Urquidi-Macdonald M. Prediction of IGSCC in type 304 SS using artificial neural networks [C] Corrosion 1994. Houston, TX: NACE 1994:103.

[5] Wang Hui, Song Bifeng, Wang Le, Lv Guozhi Three-dimensional Computational Simulation of Corrosion Pit Growth Morphology. [J] Acta Aeronautica et Astronautica Sinica, 2009 30(11): 2186-2192.

[6] Wang Hui, Lv Guozhi, Zhang You Hong, Cellular automaton simulations of corrosion pit growth.Corrosion science and protection technology. 20(6) (2008):472-475.

[7] Bastien Chopard and Michel Droz, Cellular Automaton Modeling of Physical Systems, 1st edn. The Pitt Building Trumpington Street, Cambridge CB2 1RP, United Kingdom.

[8] G.R.Liu, M.B.Liu, Smoothed particle hydrodynamics: A meshfree particle method World Scientific Press.Singpore 2003.

[9] G.R.Liu, Meshfree method Moving Beyond the Finite Element Method, CRC Press, Boca Ratou, USA, 2000.

[10] G.R.Liu, Y.T.Gu, An introduction to meshfree methods and their programming, Springer, 2005.

[11] G.R.Liu, G.Y.Zhang, K.Y.Dai, Y.Y.Wang, Z.H.Zhong, G.Y.Li, X.Han. A linearly conforming point interpolation method (LC-PIM) for 2D solid mechanics problems, Int J Computat Methods, 2005, 2(4):645-655.

[12] G.R.Liu, Y.Li, K.Y.Dai, Z.H.Zhong, G.Y.Yi, X.Han, A linearly conforming RPIM for solid mechanics problems Int J Computat Methods, 2006, 3(4):401-428.

[13] G.R.Liu, A generalized gradient smoothing technique and the smoothing bilinear form for Galerkin

formulation of a wide class of computational methods, Int J Computat Meth 2008a, 5(2):199-236.

[14] G.R.Liu, Z.Wang, G.Y.Zhang, Z.Zong, S.Wang, An Edge-based smoothed point interpolation method for material discontinuity, Mech Adv Mater Struc, 2012, 19:3-17.

[15] G.Y.Zhang, G.R.Liu, T.T.Nguyen, C.X.Song, The upper bound property for solid mechanics of the linearly conforming radial point interpolation method (LC-RPIM), International Journal of Compu, 2007,4(3):521-541.

[16] G.Y.Zhang, G.R.Liu, Y.Y.Wang, H.T.Huang, Z.H.Zhong, G.Y.Li, X.Han, A linearly conforming point interpolation method(LC-PIM) for three-dimensional elasticity problems,International Journal of Co mpu,2005,72(13):1524-1543.

[17] G.R.Liu, T.T.Nguyen, K.Y.Lam, An edge-based smoothed finite element method(ES-FEM) for static and dynamic problems of solid mechanics, J.Sound.Vib.,DOI:10.1016/j.jsv.2008.08.027.

[18] G.R.Liu, A G space theory and a weakend weak(W^2) form for a unified formulation of compatible incompatible methods: Part I Theory,Int.J.Numer.Meth.Eng.2010, 81:1093-1126.

[19] G.R.Liu, A G space theory and a weakend weak(W^2) form for a unified formulation of compatibl and incompatible methods: Part II applications to solid mechanics problems.Int.J.Numer.Meth.Eng. 2010, 81:1127-1156.

[20] G.R.Liu A weakened weak (W^2) form for a unified formulation of compatible and incompatible displacement methods, Int. J. Numer. Meth. Eng. (revised).